Reminder: Overview

Part II day 1: E- and B-modes
- Very brief reminders from day I
- E-/B-mode decomposition recap
- E-/B-mode estimators
- Galaxy-galaxy lensing: motivation

Part II day 2: Shear estimation
- Galaxy-galaxy lensing in detail
- Back to the aperture mass: Filter function relation
- Spherical-sky lensing projections
- Shear calibration

Part II day 3: Cosmological parameter estimation
- Numerical simulations
- Covariance estimation
- Likelihood and parameter estimation
- Higher-order statistics

Tangential shear and surface mass I

In an exercise you have derived the relation between tangential shear and encompassed projected surface mass,

$$\langle\gamma_\mathrm{t}\rangle(\theta) = \bar{\kappa}(\leq\theta) - \langle\kappa\rangle(\theta).$$

We will re-write equation defining the *surface mass excess* $\Delta\Sigma$.

Surface mass excess

Assume a single lens at (angular diameter) distance D_l. Approximate for this case the expression of the convergence

$$\kappa(\boldsymbol{\theta},\chi) = \frac{3}{2}\Omega_\mathrm{m}\left(\frac{H_0}{c}\right)^2\int_0^\chi \mathrm{d}\chi'\frac{(\chi-\chi')\chi'}{\chi a(\chi')}\,\delta\left(\chi'\boldsymbol{\theta},\chi'\right).$$

and write D_s for the distance of the source, and D_ls for the distance between lens and source. Write all distances as proper, not comoving distances, express the density contrast in terms of the density, $\delta = \Delta\rho/\bar{\rho}$, and use the critical density ρ_crit.

Tangential shear and surface mass II

Assume that the lens mass distribution ρ extends over the inverval $[D_\mathrm{l} - \Delta D/2; D_\mathrm{l} + \Delta D/2]$.

$$\kappa(\boldsymbol{\theta}) = \frac{4\pi G}{c^2} \frac{D_\mathrm{l} D_\mathrm{ls}}{D_\mathrm{s}} \int_{D_\mathrm{l}-\Delta D/2}^{D_\mathrm{l}+\Delta D/2} \mathrm{d}D\, \Delta\rho(D\boldsymbol{\theta}, D).$$

Define the *critical surface mass density*

$$\Sigma_\mathrm{cr}^{-1}(\theta) := \frac{4\pi G}{c^2} \frac{D_\mathrm{l} D_\mathrm{ls}}{D_\mathrm{s}}$$

to write convergence as

$$\kappa(\boldsymbol{\theta}) = \frac{\Sigma(\boldsymbol{\theta})}{\Sigma_\mathrm{cr}}. \tag{2}$$

[Why is Σ_cr called *critical* surface mass?]
With that, we define the surface mass excess

$$\Delta\Sigma(\leq\theta) := \langle\gamma_\mathrm{t}\rangle(\theta)\, \Sigma_\mathrm{cr} = \bar{\Sigma}(\theta) - \langle\Sigma\rangle(\theta).$$

Statistical galaxy-galaxy lensing (GGL) I

The convergence or tangential shear defined in the last slides depend linearly on the mass distribution ρ, or Σ. So it seems to be a first-order statistic.

However, when measured statistically using a population of foreground galaxies, it can be written as two-point correlation function. The convergence is then the correlation of background lensing convergence and foreground galaxy position.

If we write the latter as galaxy over-density δ_g, we get

$$\begin{aligned}
\langle\kappa\rangle(\theta) &= \langle\kappa(\boldsymbol{\vartheta})\delta_\mathrm{g}(\boldsymbol{\vartheta}+\boldsymbol{\theta})\rangle_{\boldsymbol{\vartheta}} \\
&= \Sigma_\mathrm{cr}^{-1}\bar{\rho}\int \mathrm{d}D\, \langle\delta(D\boldsymbol{\theta}, D)\delta_\mathrm{g}(D_\mathrm{l}\boldsymbol{\theta}, D_\mathrm{l})\rangle \\
&= \Sigma_\mathrm{cr}^{-1}\bar{\rho}\int \mathrm{d}D\, \xi_{\delta\mathrm{g}}(\sqrt{(D\theta)^2 + (D-D_\mathrm{l})^2}).
\end{aligned}$$

Statistical galaxy-galaxy lensing (GGL) II

Properties of statistical GGL

- Circular averages of tangential shear: robust against (some) systematic, e.g. large-scale modes of PSF residuals cancel out.
  CFHTLenS: 25% fields had to be discarded for cosmic shear, none for GGL.
- Simple null tests:
  $\langle\gamma_\times\rangle$ around foreground objects (parity mode, should vanish).
  $\langle\gamma_\mathrm{t}\rangle$ around random points, or special points that should not be correlated with foreground sample such as chip corners, field centres, stars.
- Higher SNR compared to cosmic shear:
  correlation with tracers of dense matter regions;
  one shape instead of two;
- Can use spectroscopic galaxies for foreground sample

Parenthesis: galaxy bias I

Simple bias

GGL measures the cross-correlation between galaxies and dark (more precisely: total) matter, $\langle\delta_\mathrm{g}\delta\rangle$. This correlation is non-zero since galaxies trace the underlying matter.
Simplest model: linear, constant, deterministic bias:

$$\delta_\mathrm{g} = b\delta.$$

From that it follws that

$$\langle\delta_\mathrm{g}\delta_\mathrm{g}\rangle(\theta) = b^2\langle\delta\delta\rangle(\theta); \qquad \langle\delta_\mathrm{g}\delta\rangle(\theta) = b\langle\delta\delta\rangle(\theta),$$

or in Fourier space

$$P_\mathrm{gg}(k) = b^2 P_\mathrm{mm}(k); \qquad P_\mathrm{gm}(k) = bP_\mathrm{mm}(k).$$

Parenthesis: galaxy bias II

Properties

- The bias depends on the galaxy properties (type, color, luminosity, ...), and can be measured for different populations (e.g. early/late-type).
- Bias is redshift-dependent. Difficult to measure since degenerate with z-dependent selection effects. Volume-limited samples: Bias tends to increase with z: galaxies are more rare objects at higher z, situated in more extreme environments (halo centres).

Sample selection for galaxy bias measurement

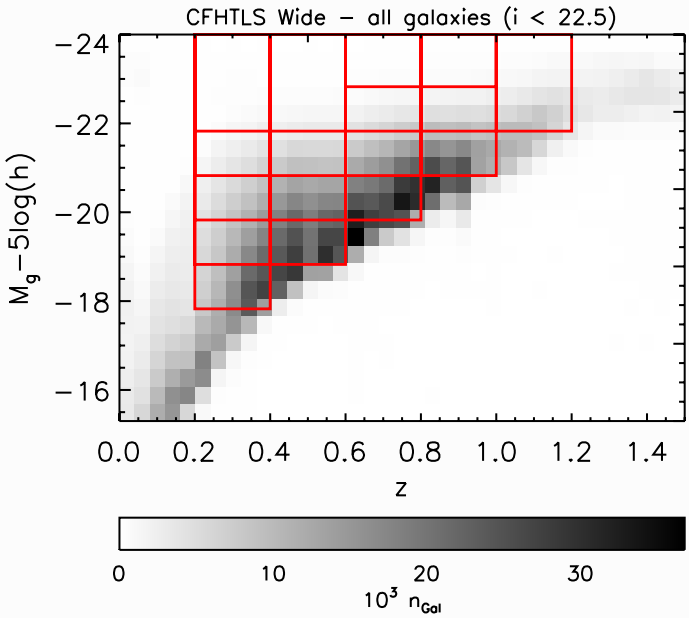

Sample selection in absolute magnitude and redshfit, from (Coupon et al. 2012).
Samples in horizontal boxes have same absolute magnitudes and are volume-limited.

Galaxy bias extended I

More complex bias models

- Scale-dependence, $b(\theta)$, or $\hat{b}(\hat{k})$. In particular on small scales, bias is not constant.
- Non-linear bias

$$\delta_\mathrm{g} = b_1\delta + b_2\delta^2 + b_3\delta^3 + \dots$$

- Stochastic bias

  Relation between δ_g is not determinstic ($\delta_\mathrm{g} = b\delta$) but stochastic. In a statistical picture, the two fields δ_g and δ can be interpreted a realizations of random fields with joint pdf $p(\delta_\mathrm{g}, \delta)$. The study of stochastic biasing is trying to quantify this joint pdf.

Galaxy bias extended II

At second-order level, one can measure the variances of both fields, and their cross-correlation. If the fields are correlated, one can write down the following two relations:

$$b = \frac{\sigma_\mathrm{g}}{\sigma} = \sqrt{\frac{\langle\delta_\mathrm{g}^2\rangle}{\langle\delta^2\rangle}}; \quad r = \frac{\sigma_\mathrm{gm}^2}{\sigma_\mathrm{g}\sigma} = \frac{\langle\delta_\mathrm{g}\delta\rangle}{\sqrt{\langle\delta_\mathrm{g}^2\delta\rangle\langle\delta^2\delta\rangle}}$$

introducing a correlation coffecient $r = -1 \dots 1$ between both fields.

In the above ratio cosmology dependence (dm correlation function or power spectrum) mainly drops out!

Allows for model-independent measurement.

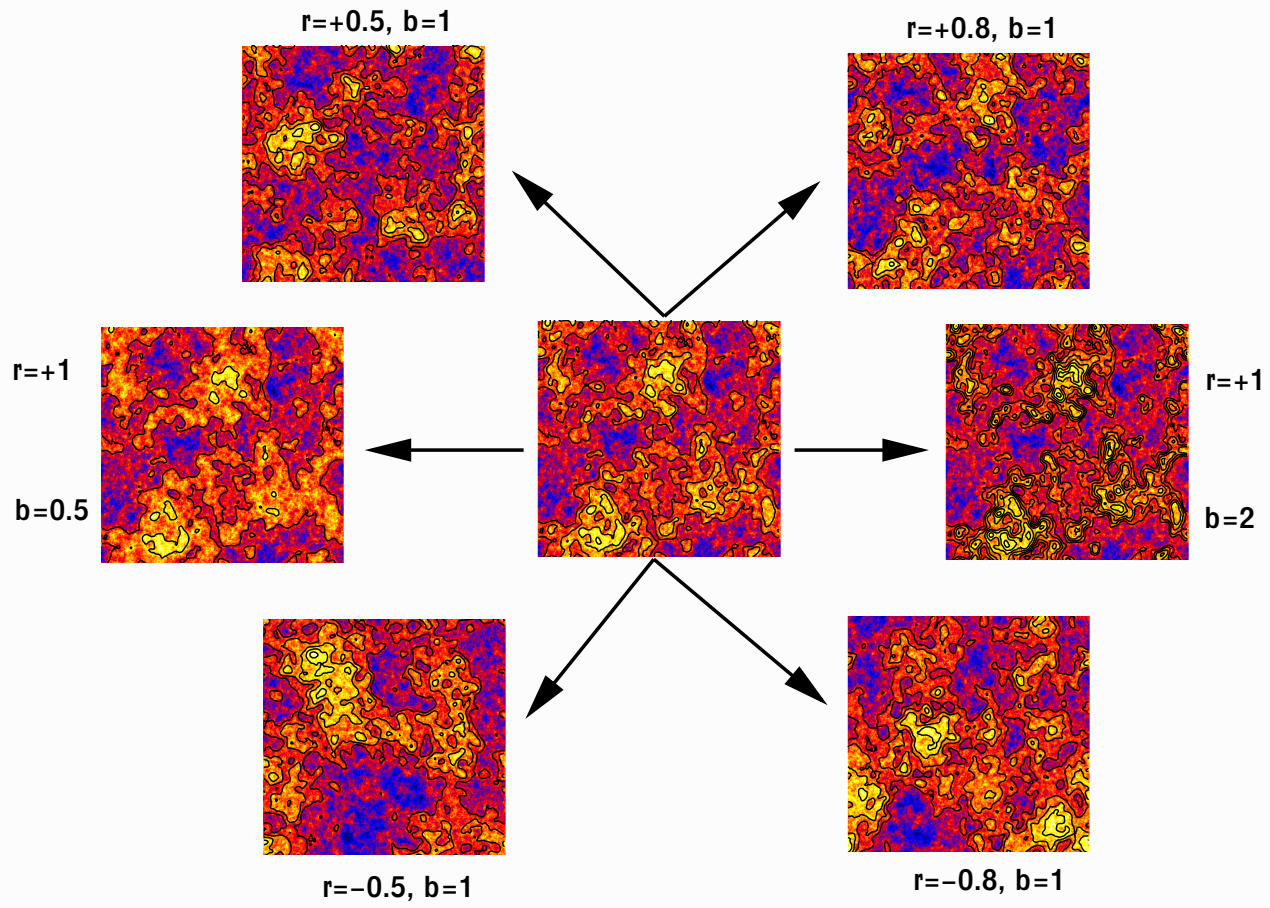

Illustration of correlated fields, from [P. Simon, PhD thesis, 2005].

Galaxy bias II

Question: How would the correlation between δ_g and δ look like for negative bias $b < 0$? For example $b = -1, r = 1$.

Non-linear and stochastic bias

A non-linear bias can mimic stochasticity.
Consider the (made-up) example of deterministic bias with $\delta_g = \delta^3$.

Exercise:

Calculate r in the case where both fields follow Gaussian pdf's.

Galaxy bias II

Question: How would the correlation between δ_g and δ look like for negative bias $b < 0$? For example $b = -1, r = 1$.

Non-linear and stochastic bias

A non-linear bias can mimic stochasticity.
Consider the (made-up) example of deterministic bias with $\delta_\mathrm{g} = \delta^3$.
Exercise:
Calculate r in the case where both fields follow Gaussian pdf's.

$$r = \frac{\langle \delta_\mathrm{g} \delta \rangle}{\sqrt{\langle \delta_\mathrm{g}^2 \delta \rangle \langle \delta^2 \delta \rangle}} = \frac{\langle \delta^4 \rangle}{\sqrt{\langle \delta^2 \rangle \langle \delta^6 \rangle}} = \frac{3\sigma^4}{\sqrt{\sigma^2 15 \sigma^6}} = \frac{3}{\sqrt{3 \cdot 5}} = \frac{3}{5} \approx 0.77 \leq 1!$$

Final note: The density field *cannot* be a Gaussian, since $\delta \leq -1$.

GGL: model-independent measurement of b/r

Idea:
Combine weak lensing and galaxy clustering to determine b and r.

- Galaxy clustering $\langle \delta_\mathrm{g}^2 \rangle$
- Galaxy-galaxy lensing $\langle \delta_\mathrm{g} \delta \rangle$
- Cosmic shear $\langle \delta^2 \rangle$

Cosmic shear is the most difficult to measure, so first measurements only used GC and GGL.

Form ratio:

$$\frac{\langle \delta_\mathrm{g} \delta \rangle(\theta)}{\langle \delta_\mathrm{g} \delta_\mathrm{g} \rangle(\theta)} = \frac{br}{b^2} = \frac{b}{r}.$$

Any cosmology-dependence, e.g. of clustering, drops out in the ratio.
These density correlations are projected to weak-lensing observables, and b and r (if constant) can directly be measured.

GGL: Aperture measures I

How can we trace the galaxy and dark-matter over-densities with weak lensing?
Use aperture measures

$$\langle N^2\rangle(\theta), \langle NM_{\rm ap}\rangle(\theta), \langle M_{\rm ap}^2\rangle(\theta)$$

to trace

$$\langle \delta_{\rm g}^2\rangle, \langle \delta_{\rm g}\delta\rangle, \langle \delta^2\rangle.$$

Difficulty: Structure along all redshifts contribute to cosmic shear $\langle M_{\rm ap}^2\rangle$, not only mass associated with foreground galaxy sample $\delta_{\rm g}$.

Solutions:

- Choose background sample such that maximum lensing efficiency coincides with foreground redshift.
- Add correction functions with minor dependency on cosmology (geometry).

Redshift calibration factors

Aperture measure ratios

$$b(\theta) = \sqrt{\frac{\langle N^2\rangle(\theta)}{\langle M_{\rm ap}^2\rangle(\theta)}} \quad ?$$

$$r(\theta) = \frac{\langle NM_{\rm ap}\rangle(\theta)}{\sqrt{\langle N^2\rangle(\theta)\langle M_{\rm ap}^2\rangle(\theta)}} \quad ?$$

Redshift calibration factors

Aperture measure ratios

$$b(\theta) = f_1(\theta)\sqrt{\frac{\langle N^2\rangle(\theta)}{\langle M_{\rm ap}^2\rangle(\theta)}}$$

$$r(\theta) = f_2(\theta)\frac{\langle NM_{\rm ap}\rangle(\theta)}{\sqrt{\langle N^2\rangle(\theta)\langle M_{\rm ap}^2\rangle(\theta)}}$$

Calibration factors f_1, f_2 to account for different redshifts/lensing efficiency (Hoekstra et al. 2001). Calculate those using theoretical model for fiducial cosmology (fixing power spectrum, geometry), setting $b = r = 1$:

$$f_1(\theta) = \left.\sqrt{\frac{\langle M_{\rm ap}^2\rangle(\theta)}{\langle N^2\rangle(\theta)}}\right|_{\rm fid,b=1}$$

$$f_2(\theta) = \left.\frac{\sqrt{\langle N^2\rangle(\theta)\langle M_{\rm ap}^2\rangle(\theta)}}{\langle NM_{\rm ap}\rangle(\theta)}\right|_{\rm fid,b=r=1}$$

Redshift calibration factors

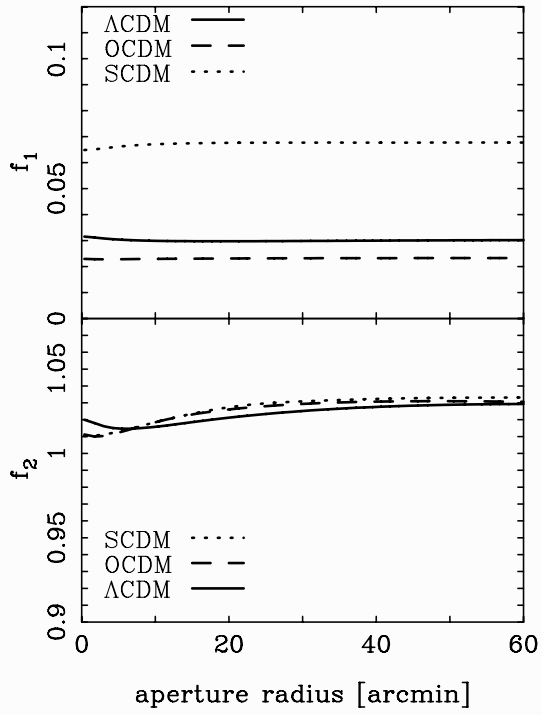

Scale-and cosmology-dependence of calibration factors. From (Simon et al. 2007), GaBoDS (Garching-Bonn Deep Survey).

GGL results: model-independent measurement of b/r

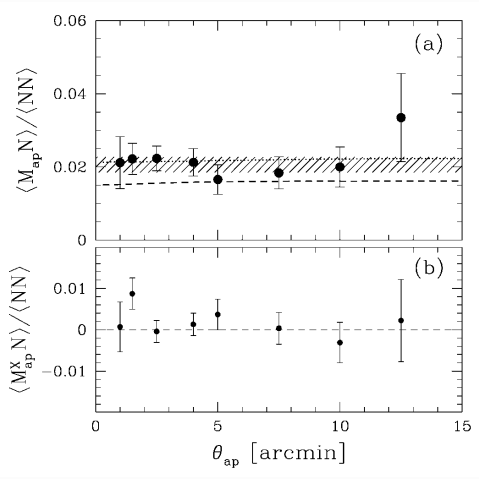

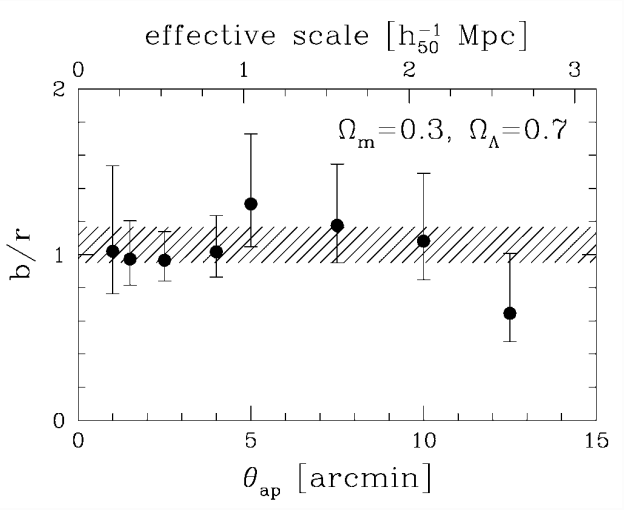

$$\mathcal{R} = \frac{r\Omega_m}{100b}[(5.8 - 1.6\Omega_m^{0.63}) + (4.6 - 2.6\Omega_m^{0.63})\Omega_\Lambda^{1.23}].$$

Observed ratio $\mathcal{R}$ (a), and B-mode (b); b/r (*right*) from (Hoekstra et al. 2001).

Main result: no scale-dependence found (on observed scales).

GGL results: model-indep. measurement of b and r I

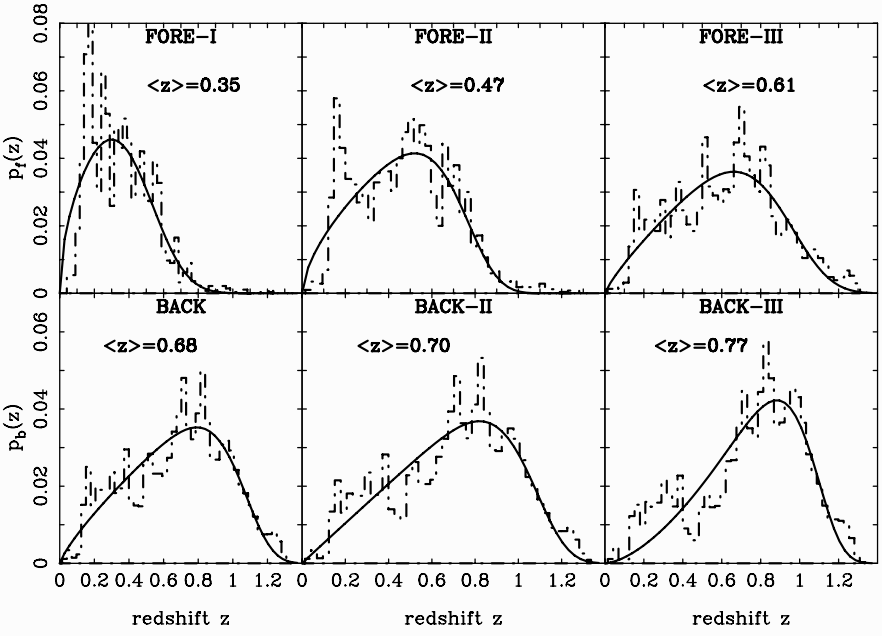

Redshift distributions for GaBoDS samples, estimated from COMBO-17. From (Simon et al. 2007), GaBoDS (Garching-Bonn Deep Survey).

GGL results: model-indep. measurement of b and r II

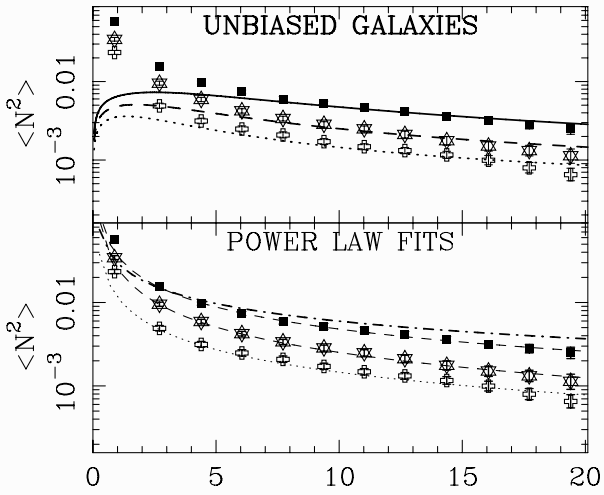

Filled boxes, open stars, open crosses = FORE-I, FORE-II, FORE-III.

Galaxy clustering: Bias on small scales is not constant, but scale-dependent. Stronger galaxy clustering than from constant bias. (Simon et al. 2007), GaBoDS (Garching-Bonn Deep Survey).

GGL results: model-indep. measurement of b and r III

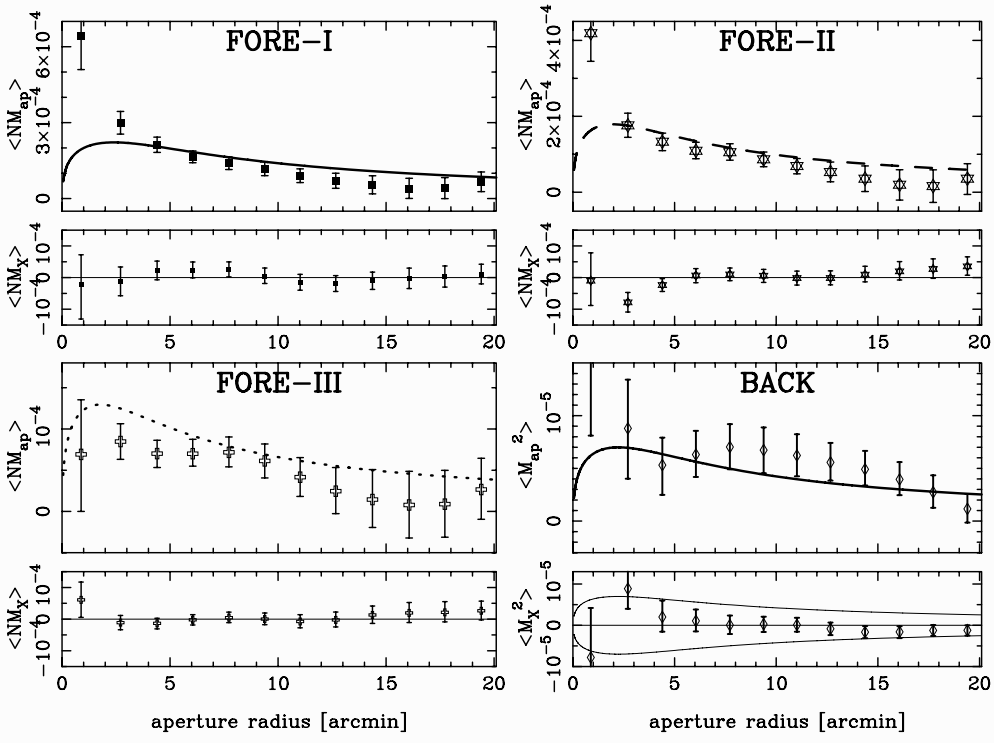

GGL and cosmic shear. (Simon et al. 2007), GaBoDS (Garching-Bonn Deep Survey).

GGL results: model-indep. measurement of b and r IV

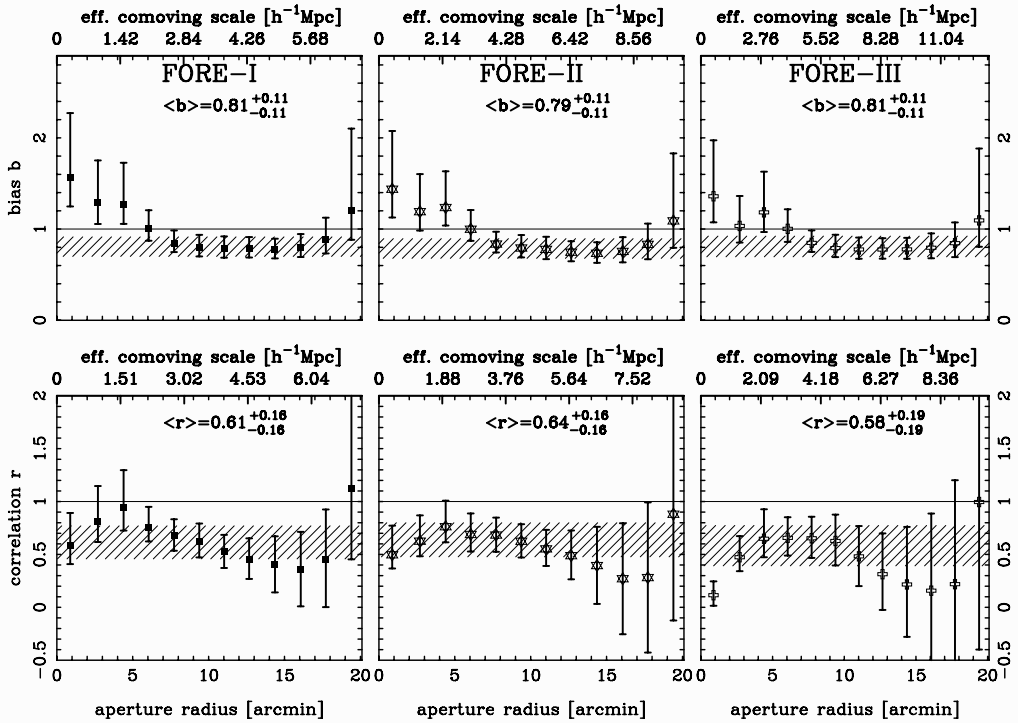

Bias and correlation coefficient. (Simon et al. 2007), GaBoDS (Garching-Bonn Deep Survey).

GGL: HOD model measurements

increasing luminosity →

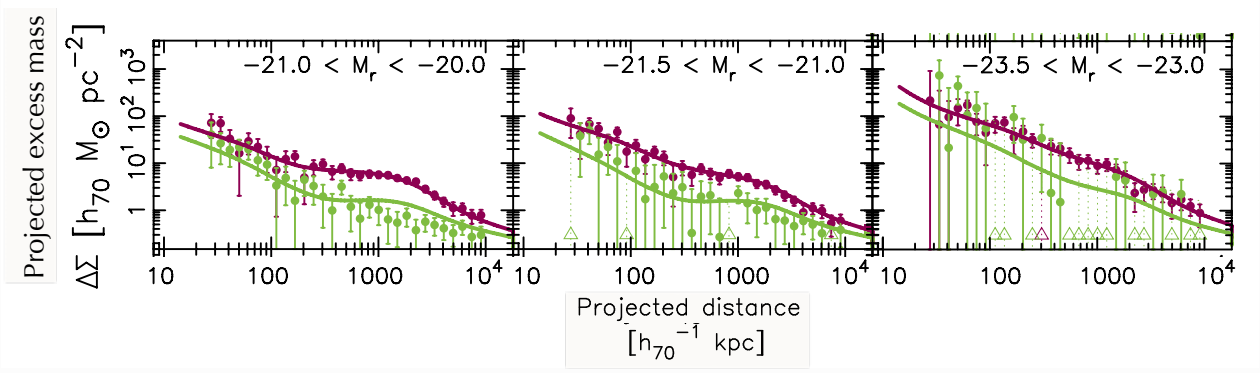

Purple=red early-type galaxies; Green=blue late-type galaxies. From (Velander et al. 2014).

GGL: HOD model measurements

increasing luminosity →

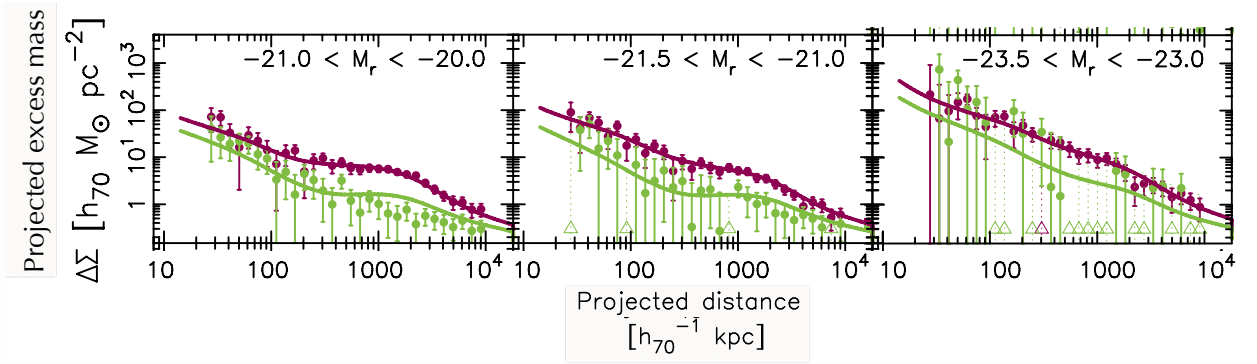

Purple=red early-type galaxies; Green=blue late-type galaxies. From (Velander et al. 2014).

- Red galaxies have larger associated mass than blue galaxies.
- Exceess mass increases with luminosity. Light traces mass.

GGL: HOD model measurements

increasing luminosity →

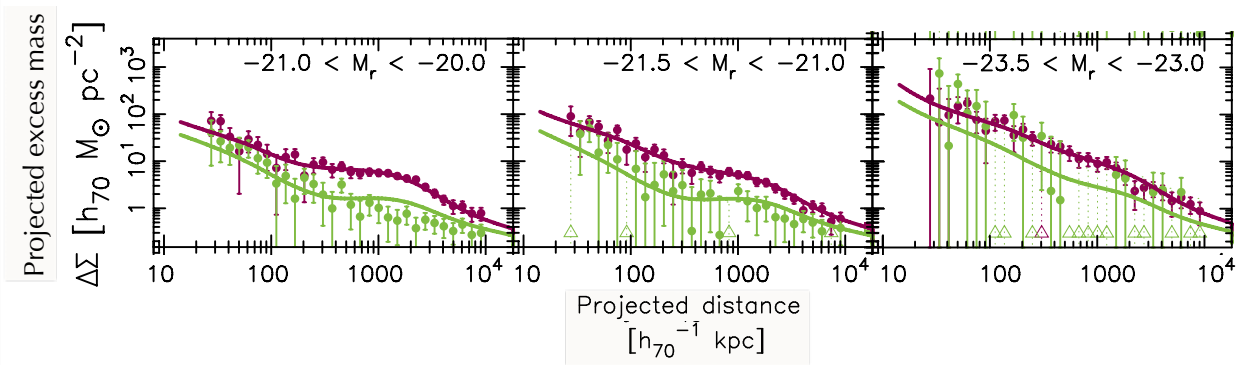

Purple=red early-type galaxies; Green=blue late-type galaxies. From (Velander et al. 2014).

- Red galaxies have larger associated mass than blue galaxies.
- Exceess mass increases with luminosity. Light traces mass.
- Bump at 1 Mpc for low-luminosity red galaxies, disappears at higher L. Red satellite galaxies.

GGL: HOD model measurements

increasing luminosity →

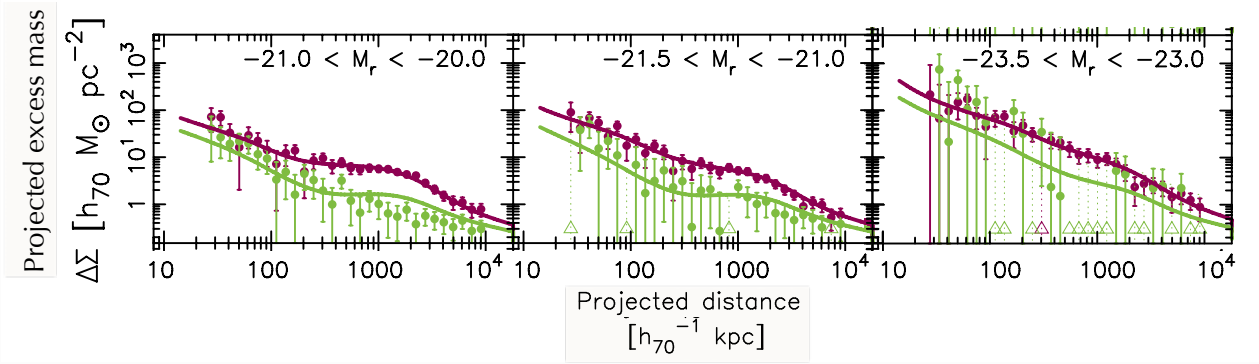

Purple=red early-type galaxies; Green=blue late-type galaxies. From (Velander et al. 2014).

- Red galaxies have larger associated mass than blue galaxies.
- Exceess mass increases with luminosity. Light traces mass.
- Bump at 1 Mpc for low-luminosity red galaxies, disappears at higher L. Red satellite galaxies.
- Bump at slightly larger scale for blue galaxies. 2-halo term, from clustered nearby galaxies.

GGL: HOD model

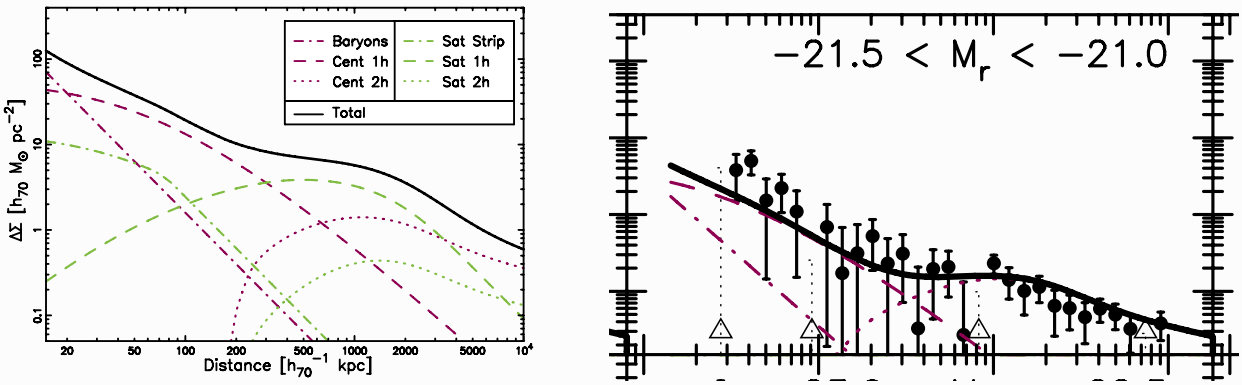

HOD model, (Velander et al. 2014).

GGL: M/L parameters

$$M_{200} = M_{0,L} \left(\frac{L}{L_{\rm fid}} \right)^{\beta_L}$$

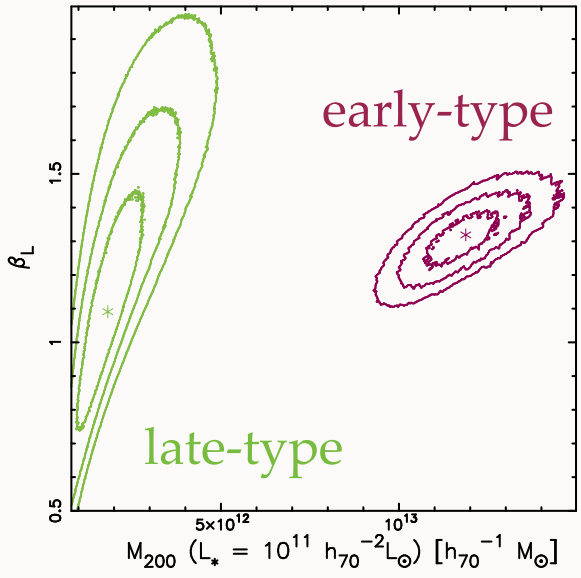

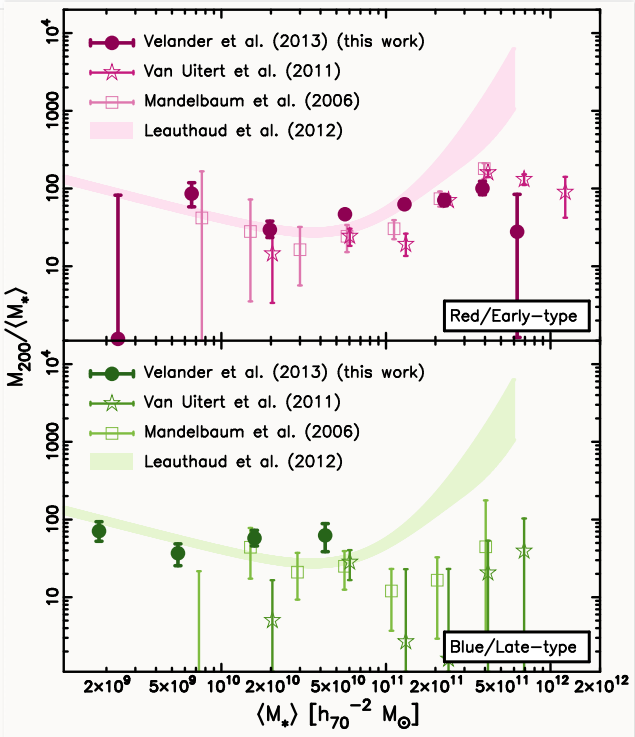

(Velander et al. 2014).

Modified gravity

General, perturbed Friedmann-Lemaître Robertson Walker (FLRW) metric:

$$\mathrm{d}s^2 = \left(1 + \frac{2\Psi}{c^2}\right) c^2 \mathrm{d}t^2 - a^2(t) \left(1 - \frac{2\Phi}{c^2}\right) \mathrm{d}l^2,$$

Valid for weak fields, (Bardeen) potentials $\Psi, \Phi \ll c^2$.

- In GR, and absence of anisotropic stress: $\Psi = \Phi$.
- In most modified gravity models: $\Psi \neq \Phi$! Very generic signature for MoG.

Some characteristics

- Ψ is Newtonian potential. Time-like. Quantifies time dilation.
- Ψ is gravitational action on non-relativistic objects (e.g. galaxies).
- Φ is space-like. Describes spatial curvature.
- $\Psi + \Phi$ is gravitational action on relativistic objects (e.g. photons; lensing!). [Photons travel equal parts of space and time. This is the origin for the factor two in GR equations compared to Newtonian mechanics!]

Testing GR I

Idea of a null test

Measure difference in potentials to test GR: Galaxy clustering for Ψ, weak lensing for $\Psi + \Phi$.

Modified Poisson equation

Potentials are related to density contrast δ via Poisson equation. Generalise to account for MoG, and write in Fourier space:

$$\begin{aligned} k^2\tilde{\Psi}(k,a) &= 4\pi G a^2 \left[1+\mu(k,a)\right]\rho\,\tilde{\delta}(k,a); \\ k^2\left[\tilde{\Psi}(k,a)+\tilde{\Phi}(k,a)\right] &= 8\pi G a^2 \left[1+\Sigma(k,a)\right]\rho\,\tilde{\delta}(k,a). \end{aligned}$$

With free parameters/functions μ, Σ. GR: $\mu = \Sigma = 0$.

Testing GR II

Probes of Bardeen potentials

Assuming linear, deterministic bias (b =const, $r = 1$).

- Galaxy clustering measures Ψ and b; $\langle\delta_\mathrm{g}^2\rangle \propto b^2 P_\Psi$.
- GGL measures $\Psi + \Phi$ and b; $\langle\delta_\mathrm{g}\delta\rangle \propto b P_{\Psi+\Phi}$.

$\rightarrow$ form ratio to get rid of cosmology dependence!
However, bias still remains, need another observable.

- RSD anisotropy parameter; $\beta = \frac{1}{b}\frac{\mathrm{d}\ln D_+(a)}{\mathrm{d}\ln a}$.

TODO: Add pi, sigma plot, equation, Samushia et al. 2014.

E_G parameter

$$E_\mathrm{G} \simeq \frac{1}{\beta}\frac{\langle\delta_\mathrm{g}\delta\rangle}{\langle\delta_\mathrm{g}^2\rangle}$$

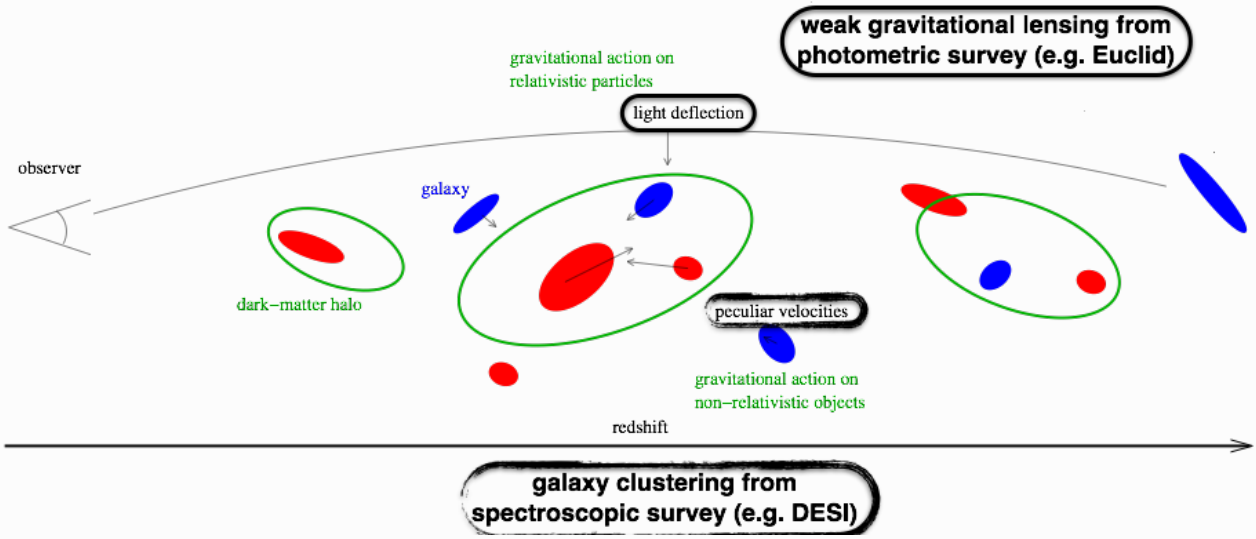

Testing GR: results I

SDSS (Reyes et al. 2010)

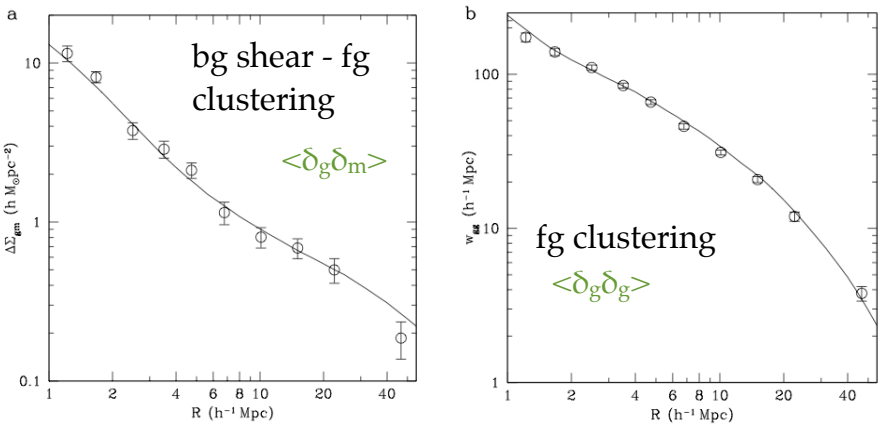

$\beta = 0.309 \pm 0.035$

from SDSS galaxy clustering (redshift-space distortions) Tegmark et al. (2006)

Testing GR: results II

Introducing new observable to exclude small scales:

$$\Upsilon_{\rm gm}(R) = \Delta\Sigma_{\rm gm}(R) - \left(\frac{R_0}{R}\right)^2 \Delta\Sigma_{\rm gm}(R_0)$$
$$= \frac{2}{R^2}\int_{R_0}^{R} {\rm d}R'\, R'\, \Sigma_{|rmgm}(R') - \Sigma_{\rm gm}(R') + \left(\frac{R_0}{R}\right)^2 \Sigma_{\rm gm}(R_0),$$

(Baldauf et al. 2010).

Define in analogy $\Sigma_{\rm gg}$.

Then modified $E_{\rm G}$ probe of gravity:

$$E_{\rm G}(R) = \frac{1}{\beta}\frac{\Sigma_{\rm gm}(R)}{\Sigma_{\rm gg}(R)}.$$

Testing GR: results III

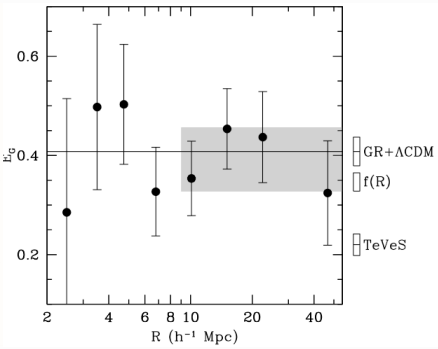

From (Reyes et al. 2010).

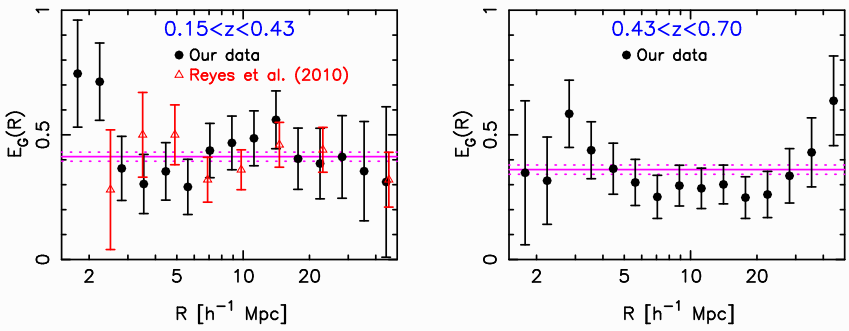

From (Blake et al. 2016).

Recall: Aperture-mass definition

Yesterday we introduced the aperture-mass as convolution of the shear field with a filter Q,

$$M_{\rm ap}(\theta,\boldsymbol{\vartheta}) = \int \mathrm{d}^2\vartheta'\, Q_\theta(|\boldsymbol{\vartheta}-\boldsymbol{\vartheta}'|)\,\gamma_{\rm t}(\boldsymbol{\vartheta}')$$

and claimed that this was equivlaent of convolving the convergence with another filter U,

$$M_{\rm ap}(\theta,\boldsymbol{\vartheta}) = \int \mathrm{d}^2\vartheta'\, U_\theta(|\boldsymbol{\vartheta}-\boldsymbol{\vartheta}'|)\,\kappa^{\rm E}(\boldsymbol{\vartheta}'), \tag{3}$$

(Kaiser et al. 1994, Schneider 1996).

Relation between U and Q I

First, place aperture at center, $\boldsymbol{\vartheta}=0$. Assume that the filter function $U_\theta(\vartheta)$ has support $[0;\theta]$, (note that θ can be ∞.)
Introduce angle-averaged convergence,

$$\langle\kappa\rangle(\vartheta) := \frac{1}{2\pi}\int_0^{2\pi}\mathrm{d}\varphi\,\kappa(\vartheta,\varphi),$$

and write aperture-mass

$$M_{\rm ap}(\theta) = \int_0^\theta \mathrm{d}\vartheta\,\vartheta\,U_\theta(\vartheta)\langle\kappa\rangle(\vartheta).$$

Integrate in parts, defining

$$\vartheta\,U_\theta(\vartheta) =: \frac{\mathrm{d}X_\theta(\vartheta)}{\mathrm{d}\vartheta} \quad\leftarrow\quad X_\theta(\vartheta) = \int_0^\vartheta \mathrm{d}\vartheta'\,\vartheta'\,U_\theta(\vartheta')$$

to get

$$M_{\rm ap}(\theta) = [X_\theta(\vartheta)\langle\kappa\rangle(\vartheta)]_0^\theta - \int_0^\theta \mathrm{d}\vartheta\,U_\theta(\vartheta)\frac{\mathrm{d}\langle\kappa\rangle(\vartheta)}{\mathrm{d}\vartheta}.$$

Relation between U and Q II

To get rid of the boundary term, we demand that U be a *compensated filter* function, i.e.

$$X_\theta(\theta) = \int_0^\theta \mathrm{d}\vartheta\, \vartheta\, U_\theta(\vartheta) = 0.$$

This means, that $M_{\rm ap}$ is not sensitive to a constant convergence κ_0.
Why?
This makes it independent of the *mass-sheat degeneracy*.

We insert the expression for the derivative of the circularly averaged convergence from the TD,

$$\frac{\mathrm{d}\langle\kappa\rangle(\vartheta)}{\mathrm{d}\vartheta} = \frac{\mathrm{d}\bar{\kappa}(\leq\vartheta)}{\mathrm{d}\vartheta} - \frac{\mathrm{d}\bar{\gamma}(\leq\vartheta)}{\mathrm{d}\vartheta} = \frac{2}{\vartheta}\langle\gamma_{\rm t}\rangle(\vartheta) - \frac{\mathrm{d}\langle\gamma\rangle(\vartheta)}{\mathrm{d}\vartheta}$$

to get

$$M_{\rm ap}(\theta) = \int_0^\theta \mathrm{d}\vartheta\, U_\theta(\vartheta)\left[\frac{2}{\vartheta}X_\theta(\vartheta)\langle\gamma_{\rm t}\rangle(\vartheta) - \frac{\mathrm{d}\langle\gamma\rangle(\vartheta)}{\mathrm{d}\vartheta}\right].$$

Relation between U and Q III

The second term is again integrated by parts. The boundary term vanishes as before and we are left with

$$M_{\rm ap}(\theta) = \int_0^\theta \mathrm{d}\vartheta\left[\vartheta\frac{2}{\vartheta^2}X_\theta(\vartheta) - \frac{\mathrm{d}X(\vartheta)}{\mathrm{d}\vartheta}\right]\langle\gamma\rangle(\vartheta).$$

This can be transformed back to the form

$$M_{\rm ap}(\theta) = \int \mathrm{d}^2\vartheta\, Q_\theta(\vartheta)\langle\gamma_{\rm t}\rangle(\vartheta)$$

and we get the relation between U and Q:

$$Q_\theta(\vartheta) = \frac{2}{\vartheta^2}\int_0^\vartheta \mathrm{d}\vartheta'\,\vartheta' U_\theta(\vartheta') - U_\theta(\vartheta).$$

Relation between U and Q IV

Some properties

- If U has finite support, so has Q. [This follows from U being compensated]. That means that aperture-mass can be obtained from shear on finite region.
  [This is not true when computing κ from γ without filters. Formally, this relation requires all of $\mathbb{R}^2$.]

Reminders: lensing potential and convergence I

On day I we defined thee lensing potential ψ at sky 2D coordinate $\boldsymbol{\theta}$ for a source galaxy at comoving distance χ, in a flat universe

$$\psi(\boldsymbol{\theta}, \chi) = \frac{2}{c^2} \int_0^\chi \mathrm{d}\chi' \frac{\chi - \chi'}{\chi\chi'} \phi(\chi'\boldsymbol{\theta}, \chi').$$

The lensing convergence κ is given by a 2D Poisson equation,

$$\kappa = \frac{1}{2}\Delta\psi.$$

We pulled the 2D Laplacian through the integral, and add the 3-component $\Delta_{\chi'\chi'}$ to yield the 3D Laplacian.
We then used the 3D Poisson equation to transform the 3D potential ϕ to the density contrast δ,

$$\Delta\Phi = \frac{3H_0^2\Omega_\mathrm{m}}{2a}\delta,$$

Reminders: lensing potential and convergence II

and obtained

$$\kappa(\boldsymbol{\theta},\chi) = \frac{3}{2}\Omega_\mathrm{m}\left(\frac{H_0}{c}\right)^2 \int_0^\chi \mathrm{d}\chi' \frac{(\chi-\chi')\chi'}{\chi a(\chi')}\,\delta\left(\chi'\boldsymbol{\theta},\chi'\right).$$

Finally, we introduced a source galaxy distribution $p(\chi)\mathrm{d}\chi = p(z)\mathrm{d}z$ to get the convergence for a population of galaxies

$$\kappa(\boldsymbol{\theta}) = \int_0^{\chi_\mathrm{lim}} \mathrm{d}\chi\, p(\chi)\,\kappa(\boldsymbol{\theta},\chi) = \int_0^{\chi_\mathrm{lim}} \mathrm{d}\chi\, G(\chi)\,\chi\,\delta\left(\chi\boldsymbol{\theta},\chi\right)$$

with the lensing efficiency

$$G(\chi) = \frac{3}{2}\left(\frac{H_0}{c}\right)^2 \frac{\Omega_\mathrm{m}}{a(\chi)} \int_\chi^{\chi_\mathrm{lim}} \mathrm{d}\chi'\, p(\chi')\frac{\chi'-\chi}{\chi'}.$$

We then introduced the variance of the convergence,

$$\langle\kappa(\boldsymbol{\vartheta}+\boldsymbol{\theta})\kappa(\boldsymbol{\vartheta})\rangle = \langle\kappa\kappa\rangle(\theta),$$

Reminders: lensing potential and convergence III

and wrote it in Fourier space to define the convergence power spectrum

$$\left\langle\hat{\kappa}(\boldsymbol{\ell})\hat{\kappa}^*(\boldsymbol{\ell}')\right\rangle = (2\pi)^2\delta_\mathrm{D}(\boldsymbol{\ell}-\boldsymbol{\ell}')P_\kappa(\ell).$$

End reminder.

Spherical transformations

The Fourier transformation is only defined on a flat space. To perform Fourier transforms on fields define on the spherical sky is fine on small scales, but breaks down on very large angles. The Fourier transform should be replaced by a *spherical harmonic transformation*.

However, we have to go back one step further: Convergence and shear are defined as second derivatives of the lensing potential,

$$\kappa = \frac{1}{2}\left(\partial_1\partial_1 + \partial_2\partial_2\right)\psi = \frac{1}{2}\nabla^2\psi;\quad \gamma_1 = \frac{1}{2}\left(\partial_1\partial_1 - \partial_2\partial_2\right)\psi;\quad \gamma_2 = \partial_1\partial_2\psi.$$

These derivatives are defined in flat space and should als be replaced on the sphere.

So, we have to start again with the lensing potential.

Lensing potential on the sphere I

The lensing potential ψ from a population of source galaxies with redshift distribution $p_i(z)$ is given, in analogy to $\kappa(\boldsymbol{\theta}$ defined above, as

$$\psi(\boldsymbol{\theta}) = \frac{2}{\mathrm{c}^2}\int_0^\infty \frac{\mathrm{d}\chi}{\chi}\Phi[\chi, \chi\boldsymbol{\theta}; \chi]\, q(\chi),,$$

where the lensing efficiency q_i is given as

$$q(\chi) = \int_\chi^{\chi_{\rm lim}} \mathrm{d}\chi'\, p(\chi')\frac{\chi'-\chi}{\chi'}.$$

[Note: On day I we defined the lensing efficienty G for the convergence, which is different from q by just the "Poisson" prefactor,

$$G(\chi) = \frac{3}{2}\left(\frac{H_0}{c}\right)^2\frac{\Omega_{\rm m}}{a(\chi)}\int_\chi^{\chi_{\rm lim}} \mathrm{d}\chi'\, p(\chi')\frac{\chi'-\chi}{\chi'} = \frac{3}{2}\left(\frac{H_0}{c}\right)^2\frac{\Omega_{\rm m}}{a(\chi)}q(\chi).]$$

Lensing potential on the sphere II

Let us now derive the angular harmonics spectrum of ψ (spherical analogue of power spectrum)
Decompose potential into spherical harmonics,

$$\psi(\boldsymbol{\theta}) = \sum_{\ell=0}^\infty\sum_{m=-\ell}^{\ell}\psi_{\ell m}\mathrm{Y}_{\ell m}(\boldsymbol{\theta}); \qquad \psi_{\ell m} = \int_{\mathbb{S}^2}\mathrm{d}\Omega\,\psi(\boldsymbol{\theta})\mathrm{Y}^*_{\ell m}(\boldsymbol{\theta}).$$

Completely analogous to CMB temperature — both ψ and T are scalar fields.

The harmonics expansion coefficient is, after insertion of the expression for ψ, and Fourier-transforming the 3D potential (note: in $\mathbb{R}^3$, not on the sphere),

$$\psi_{\ell m} = \frac{2}{c^2}\int \mathrm{d}\Omega\mathrm{Y}^*_{\ell m}(\theta,\varphi)\int_0^\infty\frac{\mathrm{d}\chi}{\chi}q(\chi)\int\frac{\mathrm{d}^3k}{(2\pi)^3}\hat{\Phi}(\boldsymbol{k};\chi)\mathrm{e}^{-\mathrm{i}\boldsymbol{k}\cdot\boldsymbol{r}}.$$

Insert spherical harmonics expansion of the plane wave basis function,

$$\mathrm{e}^{\mathrm{i}\boldsymbol{k}\cdot\boldsymbol{r}} = 4\pi\sum_{\ell=0}^\infty\sum_{m=-\ell}^{\ell}\mathrm{i}^\ell\,\mathrm{j}_\ell(k\chi)\mathrm{Y}_{\ell m}(\theta,\varphi)\mathrm{Y}_{\ell m}(\theta_k,\varphi_k),$$

Lensing potential on the sphere III

and make use of orthogonality relation of the spherical harmonics

$$\int \mathrm{d}\Omega \mathrm{Y}_{\ell m}(\theta,\varphi)\mathrm{Y}^*_{\ell' m'}(\theta,\varphi) = \delta_{\ell\ell'}\delta_{mm'},$$

to yield

$$\psi_{\ell m} = \frac{\mathrm{i}^\ell}{c^2\pi^2}\int_0^\infty \frac{\mathrm{d}\chi}{\chi} q(\chi) \int \mathrm{d}^3k\, \hat{\Phi}(\boldsymbol{k};\chi)\mathrm{j}_\ell(k\chi)\mathrm{Y}_{\ell m}(\theta_k,\varphi_k).$$

Angular harmonics (cross-)spectrum (between redshift bins i and j) of the lensing potential is defined as

$$\left\langle \psi_{\ell m,i}\, \psi^*_{\ell' m',j} \right\rangle = \delta_{\ell\ell'}\delta_{mm'}C^\psi_{ij}(\ell).$$

Using once more the orthogonality of the $\mathrm{Y}_{\ell m}$'s, we get finally

$$\begin{aligned} C^\psi_{ij}(\ell) &= \frac{8}{c^4\pi}\int_0^\infty \frac{\mathrm{d}\chi}{\chi} q_i(\chi)\int_0^\infty \frac{\mathrm{d}\chi'}{\chi'} q_j(\chi')\int \mathrm{d}k k^2\, \mathrm{j}_\ell(k\chi)\mathrm{j}_\ell(k\chi')P_\Phi(k;\chi,\chi') \\ &= \frac{8}{\pi}\left[\frac{3}{2}\Omega_\mathrm{m}\left(\frac{H_0}{c}\right)^2\right]^2 \int_0^\infty \frac{\mathrm{d}\chi}{\chi}\frac{q_i(\chi)}{a(\chi)}\int_0^\infty \frac{\mathrm{d}\chi'}{\chi'}\frac{q_j(\chi')}{a(\chi')}\int \frac{\mathrm{d}k}{k^2}\,\mathrm{j}_\ell(k\chi)\mathrm{j}_\ell(k\chi')P_\mathrm{m}(k;\chi,\chi'); \end{aligned}$$

Shear on the sphere I

Preparation

Define complex derivative operator

$$\partial := \partial_1 + \partial_2.$$

From that we get

$$\partial\partial = \partial_1\partial_1 - \partial_2\partial_2 + 2\mathrm{i}\partial_1\partial_2.$$

Thus, we can rewrite the shear

$$\gamma_1 = \frac{1}{2}\left(\partial_1\partial_1 - \partial_2\partial_2\right)\psi; \quad \gamma_2 = \partial_1\partial_2\psi.$$

in complex form

$$\gamma = \frac{1}{2}\partial\partial\psi; \quad \gamma^* = \frac{\partial^*}{\partial}\psi.$$

The corresponding derivative on the sphere is called *edth* derivative $\bar{\partial}$ (Castro et al. 2005).

Shear on the sphere II

We write

$$\gamma(\boldsymbol{\theta}) = \frac{1}{2}\,\eth\,\eth\,\psi(\boldsymbol{\theta}); \quad \gamma^*(\boldsymbol{\theta}) = \frac{1}{2}\,\eth^*\,\eth^*\psi(\boldsymbol{\theta}).$$

Inserting the spherical harmonics expansion of $\psi \rightarrow 2^{\text{nd}}$ edth derivatives of $\mathrm{Y}_{\ell m}$.
This defines a new object, the *spin-weighted spherical harmonics* ${}_2\mathrm{Y}_{\ell m}$.
[Note: Spin $s = 2$ because second-derivatives; each derivative $\eth\,(\eth^*)$ raises (lowers) spin by one.]
Therefore,

$$(\gamma_1 \pm \mathrm{i}\gamma_2)(\boldsymbol{\theta}) = \sum_{\ell m} {}_{\pm 2}\gamma_{\ell m}\ {}_{\pm 2}\mathrm{Y}_{\ell m}(\boldsymbol{\theta});$$

$${}_2\gamma_{\ell m} = \int_{\mathbb{S}^2} \mathrm{d}\Omega\,\gamma(\boldsymbol{\theta})\ {}_2\mathrm{Y}^*_{\ell m}(\boldsymbol{\theta});$$

$${}_{-2}\gamma_{\ell m} = \int_{\mathbb{S}^2} \mathrm{d}\Omega\,\gamma^*(\boldsymbol{\theta})\ {}_{-2}\mathrm{Y}^*_{\ell m}(\boldsymbol{\theta}).$$

Shear on the sphere III

These objects ${}_{\pm 2}\gamma_{\ell m}$ are eigen functions of $\eth$:

$$\text{ł}(\ell, s)\ {}_s\mathrm{Y}_{\ell m}(\boldsymbol{\theta}) = \eth\,{}^2\mathrm{Y}_{\ell m}(\boldsymbol{\theta}); \quad \text{ł}(\ell, s)\ {}_{-s}\mathrm{Y}_{\ell m}(\boldsymbol{\theta}) = (\eth^*)^2\,\mathrm{Y}_{\ell m}(\boldsymbol{\theta}).$$

with the spin pre-factor (Bernardeau et al. 2012)

$$\text{ł}(\ell, 2) = \sqrt{\frac{(\ell+2)!}{(\ell-2)!}} = \sqrt{(\ell-1)\ell(\ell+1)(\ell+2)},$$

And we get the relation between shear and potential coefficients,

$${}_{\pm 2}\gamma_{\ell m} = \frac{1}{2}\text{ł}(\ell, 2)\psi_{\ell m}.$$

Shear on the sphere IV

Now it is easy to write down the shear angular harmonics spectrum, again for bins i and j to be general:

$$C_{ij}^{\gamma}(\ell) = \frac{2}{\pi}\, t^2(\ell,2) \left[\frac{3}{2}\Omega_{\rm m}\left(\frac{H_0}{c}\right)^2\right]^2 \int_0^\infty \frac{{\rm d}\chi}{\chi}\frac{q_i(\chi)}{a(\chi)} \int_0^\infty \frac{{\rm d}\chi'}{\chi'}\frac{q_j(\chi')}{a(\chi')} \times \int_0^\infty \frac{{\rm d}k}{k^2}\, P_{\rm m}(k,\chi,\chi')\, {\rm j}_\ell(k\chi)\, {\rm j}_\ell(k\chi')$$

Flat-sky approximation

Going back to flat sky from the full spherical expression, we replace again the edth by the ordinary flat-space derivatives.
(Hu 2000) calculates the derivatives of the spherical harmonics as

$$\ell^2\, {}_{\pm2}{\rm Y}_{\ell m}(\theta,\varphi) \approx {\rm e}^{\mp 2{\rm i}\phi_\ell}(\partial_1 \pm {\rm i}\partial_2)^2\, {\rm Y}_{\ell m}(\theta,\varphi)$$

and we get a slightly different expression for the shear power spectrum, with the replacement

$$t^2(\ell,2) = (\ell-1)\ell(\ell+1)(\ell+2) \to \ell^4.$$

[Note: this is a slightly strange approach, since we first expand the field into spherical harmonics, and then perform the flat-sky approximation of the derivatives. More consistent would be to start with the Fourier transform. But I don't know how to derive the ℓ^4 factor in this case without making additional assumptions, see later.]

Limber approximation I

In short:
We use the identity of the Bessel functions

$$\mathrm{j}_\ell(x) = \sqrt{\frac{\pi}{2x}}\mathrm{J}_{\ell+1/2}(x)$$

and replace Bessel function $\mathrm{J}_{\ell+1/2}(k\chi)$ by a Dirac delta $\delta_\mathrm{D}(\ell - k\chi)$ (maximum of Bessel function).
Thus:

- Only modes $\ell + 1/2 \approx k\chi$ contribute.
- Only modes at $\chi \approx \chi'$ contribute.
  We knew this already from linear perturbation theory, which holds on large scales:
  There, the density contrast scales with the linear growth factor,

$$\hat{\delta}(\boldsymbol{k}, \chi) = D_+(\chi)\hat{\delta}_0(\boldsymbol{k}) \to P_\delta(k, \chi, \chi') = D_+^2(\chi)P_{\delta,0}(k).$$

  $\to$ comoving integrals separate.

Limber approximation II

The shear harmonic spectrum then simplifies to:

$$C_{ij}^\gamma(\ell) = t^2(\ell, 2)\left[\frac{3}{2}\Omega_\mathrm{m}\left(\frac{H_0}{c}\right)^2\right]^2 \int_0^\infty \frac{\mathrm{d}k}{k^3}$$
$$\times \int_0^\infty \frac{\mathrm{d}\chi}{\chi^{3/2}}\frac{q_i(\chi)}{a(\chi)}\delta_\mathrm{D}(\ell + 1/2 - k\chi)\int_0^\infty \frac{\mathrm{d}\chi')}{\chi'^{3/2}}\frac{q_j(\chi')}{a(\chi')}\delta_\mathrm{D}(\ell + 1/2 - k\chi')\, P_\mathrm{m}(k, \chi$$

The comoving integrals are solved trivially with the Dirac delta, yielding a further k^{-2} due to a variable transformation $\mathrm{d}\chi = \mathrm{d}(k\chi)/k$.
We then substitute $(\ell + 1/2)^3 = (k\chi)^3$, and perform another variable transformation
$\mathrm{d}k\, k^{-2} = \mathrm{d}[(\ell + 1/2)\chi^{-1}]k^{-2} = (\ell + 1/2)\mathrm{d}\chi\chi^{-2}k^{-2} = \mathrm{d}\chi(\ell + 1/2)^{-1}$, and get

$$C_{ij}^\gamma(\ell) = \frac{t^2(\ell, 2)}{(\ell + 1/2)^4}\left[\frac{3}{2}\Omega_\mathrm{m}\left(\frac{H_0}{c}\right)^2\right]^2 \int \mathrm{d}\chi \frac{q_i(\chi)q_j(\chi)}{a^2(\chi)} P_\mathrm{m}\left(\frac{\ell + 1/2}{\chi}; \chi\right).$$

Approximations accuracy I

Most pre-2014 used the flat-sky approximation ($l^2(\ell, 2) \approx \ell^4$) and further $\ell + 1/2 \approx \ell$. Then the prefactor cancels.

This *standard Limber* approximation is accurate to 1% (10%) for $\ell < 60(4)$.

The next logical approximation is *extended Limber*, with $\ell + 1/2$ kept in prefactor and power-spectrum argument. This is actually a worse approximation than standard Limber, since the approximated prefactor converges only with $\mathcal{O}(\ell^1)$.

Better is *hybrid*, with ℓ in prefactor denominator, but $\ell + 1/2$ in integral.

Even better is *second-order Limber*.

Approximations accuracy II

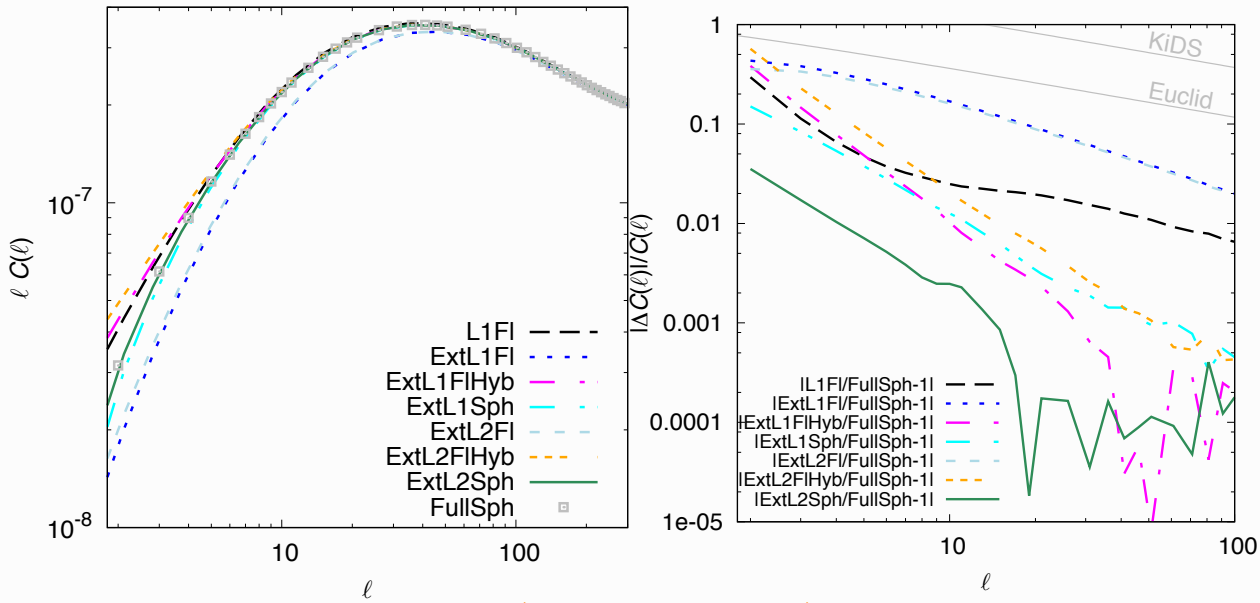

From (Kilbinger et al. 2017).

Spherical correlation function I

For the correlation function on the sphere, the Bessel functions $\mathrm{J}_{0,4}$ are replaced by the *reduced Wigner D-matrices*,

$$\xi_+(\theta) = \frac{1}{4\pi}\sum_{\ell=2}^{\infty}(2\ell+1)C^\gamma(\ell)\mathrm{d}^\ell_{2\,2}(\theta); \quad \xi_0(\theta) = \frac{1}{4\pi}\sum_{\ell=2}^{\infty}(2\ell+1)C^\gamma(\ell)\mathrm{d}^\ell_{2\,-2}(\theta).$$

These are defined as follows:

$$\begin{aligned} D^\ell_{ss'}(\alpha,\beta,-\gamma) &= \sum_m \frac{4\pi}{2\ell+1}\,{}_s\mathrm{Y}^*_{\ell m}(\theta,\varphi)\,{}_{s'}\mathrm{Y}^*_{\ell m}(\theta',\varphi') \\ &= \exp^{-\mathrm{i}s'\alpha}\, d^\ell_{ss'}(\beta)\exp^{\mathrm{i}s\gamma}. \end{aligned}$$

Angles:
β = angle between (θ,φ) and (θ',φ').
$\alpha[\gamma]$: angle to rotate $\hat{e}_\theta$ about (θ,φ) $[(\theta',\varphi')]$ perpendicular to connecting line between (θ,φ) and (θ',φ').
(Chon et al. 2004).

Spherical correlation function II

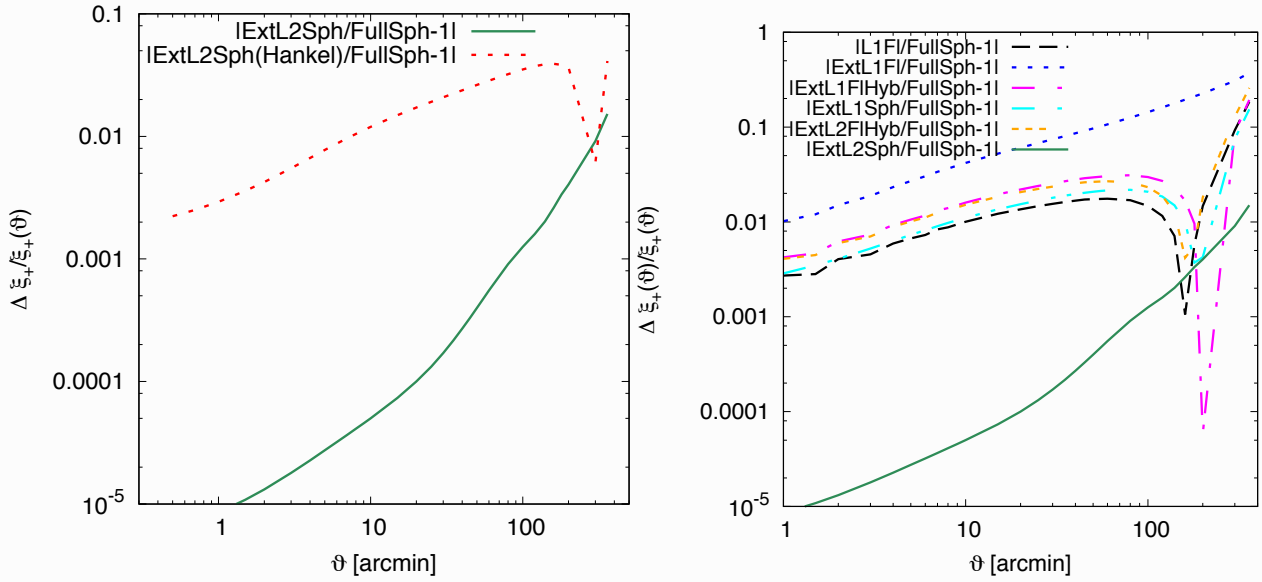

From (Kilbinger et al. 2017).

Shear bias

For ~~basically~~ all shape measurement methods: observed shear ≠ true shear.
This is called shear bias.
Reminder: Write as multiplicative and additive bias:

$$\langle \varepsilon_i^{\rm obs} \rangle = \gamma_i^{\rm obs} = (1+m_i)\gamma_i^{\rm true} + c_i; \quad i = 1,2.$$

There is also ellipticity bias, which is different:

$$\varepsilon_i^{\rm obs} = (1+m_i')\varepsilon_i^{\rm true} + c_i'; \quad i = 1,2.$$

Typical values:

year	program	m	c	$\sigma(c)$
2006	STEP I	0.1		10^{-3}
2012	CFHTLenS	0.06	0.002	
2013	great3	0.01	10^{-3}	
2014	DES	0.03–0.04	10^{-3}	
2016	KiDS	0.01–0.02	$8 \cdot 10^{-4}$	
2021	Euclid required	$2 \cdot 10^{-3}$	$5 \cdot 10^{-4}$	

Shear bias and simulations I

From the STEP I shear measurement challenge (Heymans et al. 2006).

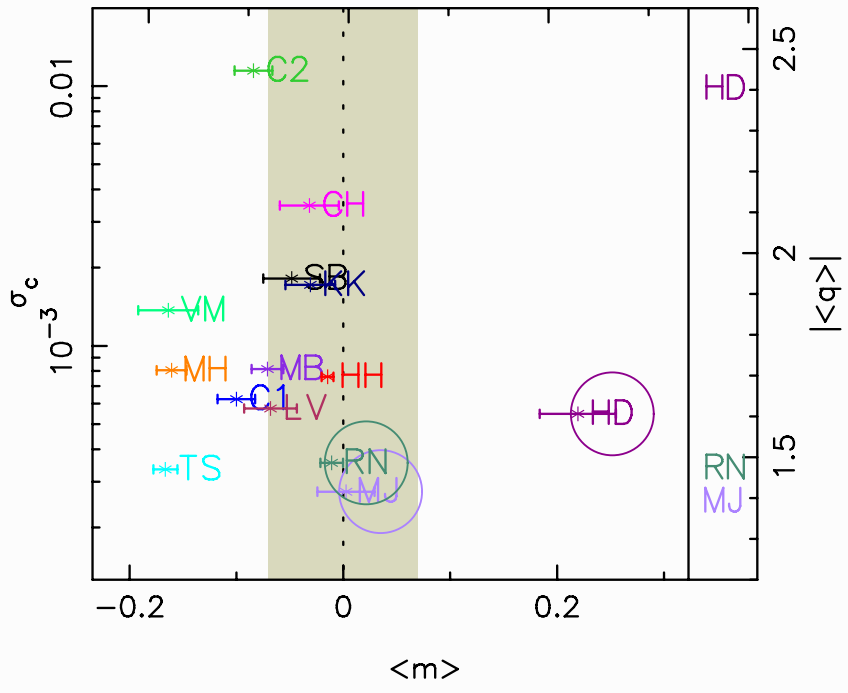

Shear bias and simulations II

From the great3 shear measurement challenge (Mandelbaum et al. 2015).

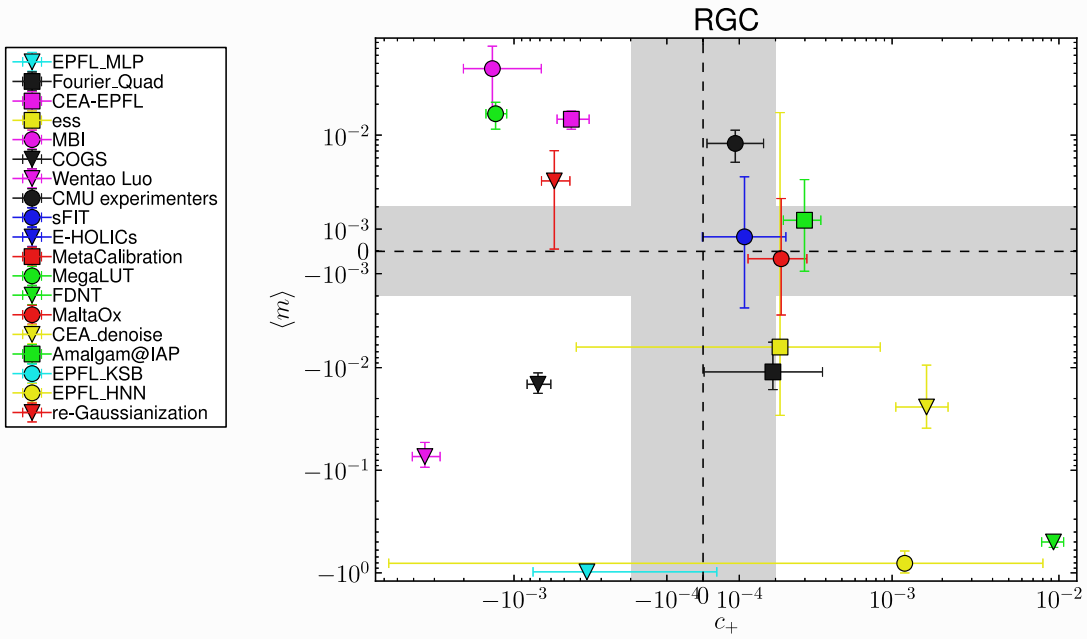

Shear bias and simulations III

Interprete with caution!

- Small biases because simulations are not realistic enough? E.g. constant PSF, analytical galaxy light distributions, simplistic noise, (constant shear)
- Simulation (challenges) only address part of the problem. Usually no blended galaxy images, star-galaxy separation, color effects, ...
- Calibrated or un-calibrated?

Amplitude of m, c not that important, since they can be calibrated emirically. What counts are $\Delta m, \Delta c$ after calibration!

More on this in a few slides.

Shear bias and simulations IV

A very general statement (see Part I day 2):

Most ellipticity estimators are non-linear pixel light distribution. Noise then creates biases in the estimator. This is called noise bias.

Thus, observed shear needs to be de-biased (calibrated) using simulations.

There are a few unbiased estimators:

- Not normalised to total flux: maybe unbiased, but very large variance
- Bayesian estimators, sample posterior distribution, unbiased if correct model, likelihood and prior.
  Prior needs to be estimated from simulations or deep survey!

Sources of bias

Reminder:

- Noise bias
- Model bias
  - Model-fitting method: incorrect model, complex galaxy morphology
  - Direct estimation: inappropriate filter function for weighted moments; truncated eigenfunction decomposition
  - Ellipticity gradients
  - Color gradients
- PSF residuals
- CTI (charge transfer inefficiency)
- Selection effects (population biases). Detection probability depends on ellipticity, orientation with PSF, pixel scale
- New: Environmental effects
  - Unresolved faint galaxies

Shear calibration

The bias should be *robust* for method to be *calibratable*.
Define *sensitivity* as dependence of bias with respect to parameters, or

$$|\partial m/\partial p_i|, \quad \text{for} \boldsymbol{p} = \text{set of parameters.}$$

A method is calibratable, see (Hoekstra et al. 2016), if

- the sensitivity is small (otherwise simulation sampling in p too costly)
- does not depend on too many parameters
- those parameters can be measured accurately (e.g. intrinsic ellipticity dispersion σ_ε from Euclid Deep Survey $\rightarrow$ requirement on accuracy of measured σ_ε sets area of calibration fields)
- those parameters can be reasonably simulated to estimate sensitivity
- difficult if parameter is correlted with shear signal (e.g. local galaxy density with large-scale structure, correlated with shear signal, magnification)

Shear calibration: Unresolved faint galaxies I

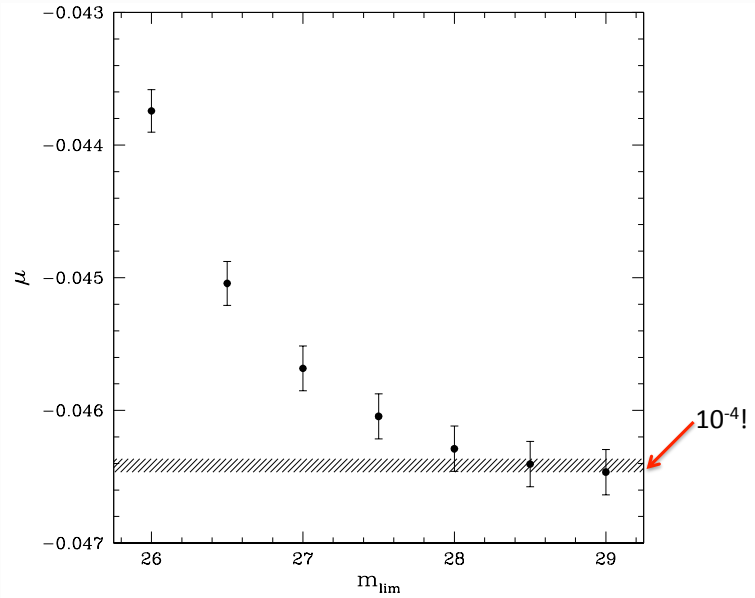

Multiplicative bias m (here μ) for galaxies $20 < m < 24.5$ as function of limiting magnitude of simulated galaxies. From (Hoekstra et al. 2016).

Overall values on y-axis (amplitude of m) not really important, will be corrected for.

Need simulation up to very high depth, until plateau in m is reached ($\partial m/\partial m_{\rm lim} = 0$).

Error bars need to decrease to match hashed region.

Shear calibration: Unresolved faint galaxies II